An Optimized Algebraic Basis for Molecular Potentials†

Andrea Bordoni* and Nicola Manini

Dipartimento di Fisica, Università di Milano, Via Celoria 16, 20133 Milano, Italy

Received: July 27, 2007; In Final Form: October 4, 2007

The computation of vibrational spectra of diatomic molecules through the exact diagonalization of algebraically determined matrices based on powers of Morse coordinates is made substantially more efficient by choosing a properly adapted quantum mechanical basis, specifically tuned to the molecular potential. A substantial improvement is achieved while still retaining the full advantage of the simplicity and numerical light-weightedness of an algebraic approach. In the scheme we propose, the basis is parametrized by two quantities which can be adjusted to best suit the molecular potential through a simple minimization procedure.

1. Introduction

In a previous work,[1] an algebraic method for the computation of vibrational spectra of diatomic molecules was introduced. Although this is a one-dimensional (1D) problem, thus an in principle trivial task, the algebraic method shows substantial advantages over both the real-space grid solution of the Schrödinger equation and harmonic-oscillator-based techniques. These advantages are especially important for extensions to the multidimensional problem of polyatomic vibrations.

The expansion of the molecular potential in powers of the Morse-potential-related quantity $v(x) = e^{-\alpha(x-x_0)} - 1$, namely

$$V_d(x) = \sum_{k=2}^{N_{max}} a_k (v(x))^k \tag{1}$$

allows an efficient and accurate approximation of a well-behaved molecular potential in the whole energy range, from the minimum region to the dissociation threshold, generally involving a moderate number of $N_{max} + 1$ parameters a_2, ...,α and x_0. Even potentials substantially distorted with respect to the Morse potential can be treated successfully. With the potential expressed in the form of eq 1, the complete Hamiltonian

$$\hat{H} \equiv \frac{\hat{p}_x^2}{2\mu} + V_d(x) \tag{2}$$

(here, μ is the reduced mass of the two-body problem, and x is the radial coordinate) can be represented on a quantum mechanical basis of choice.

The accuracy and efficiency of the direct diagonalization methods rely both on the accuracy of the potential approximation of eq 1 and on the properties of the selected basis. The basis had better be complete but also manageable, that is, related to the algebraic properties of $v(x)$, so that the evaluation of the matrix elements can be done rapidly and without approximations; this will be needed especially in view of extensions to polyatomic molecules.

2. The Basis

Previous research[1−3] showed that the basis

$$\phi_n(y) = \sqrt{\frac{\alpha n!}{\Gamma(2\sigma + n)}} y^\sigma e^{-(y/2)} L_n^{2\sigma-1}(y) \qquad \sigma > 0,\ n = 0, 1, 2, ..., \tag{3}$$

with

$$y(x) = (2s + 1)e^{-\alpha(x-x_0)} \tag{4}$$

and where L_n^ρ are generalized Laguerre polynomials can be usefully employed in general diatomic contexts, with the special choice of

$$\sigma = s - [s] \tag{5}$$

where $[s]$ indicates the integer part of s and with s related to the Morse term $a_2(v(x))^2$ in the potential expansion (eq 1), by

$$s = \frac{\sqrt{2\mu a_2}}{\hbar\alpha} - \frac{1}{2} \tag{6}$$

With the conditions of eqs 5 and 6, the basis (eq 3) was named the quasi number state basis (QNSB).[2] In the present work, we only assume that α and x_0 in eqs 3 and 4 are the same as those in the potential expansion (eq 1) and that $\sigma > 0$ and $s > -(1/2)$, but we release all additional unnecessary conditions on σ and s, for example, those expressed by eqs 5 and 6 or the condition defined by Tennyson and Sutcliffe[4,5] (TS)

$$\sigma = \frac{[2s] + 2}{2} \tag{7}$$

with s fixed by eq 6. Equation 3 thus defines a (s,σ)-parametrized family of bases, generalized QNSB (GQNSB), all sharing the following main features: (i) the basis (eq 3) is complete; (ii) the kinetic and potential operators can be written in terms of generalized ladder operator, as specified below, so that (iii) the matrix elements of a vast class of relevant operators is computable easily and exactly by means of simple algebraic relations.[1]

Even though all infinite GQNSBs are substantially equivalent, regardless of s and σ, different bases characterized by different values of s and σ show different performances when truncated to a finite number N_s of states and applied to a given quantum mechanical problem specified by μ, α, a_2, a_3, ...,$a_{N_{max}}$. Indeed,

† Part of the "Giacinto Scoles Festschrift".

* To whom correspondence should be addressed. E-mail: andrea.bordoni@unimi.it.

10.1021/jp075961f CCC: $37.00
Published on Web 11/13/2007

the purpose of the present work is to demonstrate that a properly chosen truncated GQNSB can improve the efficiency of the computation substantially, compared to earlier choices.[1,4]

3. Matrix Elements

We follow here the same approach[1] derived from supersymmetric quantum mechanics.[2,6] We introduce the generalized Morse ladder operators[1,2]

$$\hat{A}(q) = q\hat{I} - \frac{\hat{y}}{2} + \frac{i}{\hbar\alpha}\hat{p}_x$$
$$\hat{A}^\dagger(q) = q\hat{I} - \frac{\hat{y}}{2} - \frac{i}{\hbar\alpha}\hat{p}_x \quad (8)$$

parametrized by the real quantity q.[7] These operators, with a suitable choice of q, act on the states (eq 3) of the GQNSB as ladder operators

$$\hat{A}(\sigma + n)\phi_n = C_n\phi_{n-1}$$
$$\hat{A}^\dagger(\sigma + n)\phi_n = C_{n+1}\phi_{n+1} \quad (9)$$

where

$$C_n = \sqrt{n(n + 2\sigma - 1)} \quad (10)$$

According to eqs 8 and 9, σ links the parametrized basis (eq 3) to the corresponding family of generalized ladder operators. Thus, each and every basis of the form of eq 3 can be managed algebraically in this formalism for any given choice of $\sigma > 0$. In practice, the eigenfunctions (eq 3) depend explicitly on s, α, and x_0, besides σ. We fix x_0 to the position of the minimum of the potential (eq 1), as it would not provide a substantial advantage to do otherwise. Likewise, we select for α the same value as that in the potential expansion because, otherwise, all relevant matrix representations would be dense rather than sparse.[8] With these constraints on x_0 and α, an arbitrary s can be usefully employed in the basis definition; for any s value, the momentum operator p_x and the multiplication operator $e^{-\alpha(\hat{x}-x_0)}$ can be written in terms of the ladder operators (eq 8)

$$e^{-\alpha(\hat{x}-x_0)} = \frac{2q\hat{I} - [\hat{A}^\dagger(q) + \hat{A}(q)]}{(2s+1)} \quad (11)$$

$$\hat{p}_x = \frac{\hbar\alpha}{2i}[\hat{A}(q) - \hat{A}^\dagger(q)] \quad (12)$$

where the $\hat{A}$ operators also depend implicitly on the s parameter appearing in the definition (eq 4) of $\hat{y}$. On the GQNSB (eq 3), the matrix elements of any physical operator expressed as a polynomial of $e^{-\alpha(\hat{x}-x_0)}$ and p_x can be computed algebraically since eqs 11 and 12 express them in terms of the ladder operators of the corresponding specialized basis. Here, we explicitly derive the algebraic form of the Morse Hamiltonian for the general q and s.

Using eq 12, the kinetic operator $\hat{K} = (\hat{p}_x^2/2m)$ becomes

$$\hat{K} = -\frac{\hbar^2\alpha^2}{8m}[\hat{A}^2(q) + \hat{A}^{\dagger 2}(q) - \hat{A}(q)\hat{A}^\dagger(q) - \hat{A}^\dagger(q)\hat{A}(q)] \quad (13)$$

By applying the commutation relations

$$[\hat{A}(q),\hat{A}^\dagger(q')] = (q + q')I - (\hat{A}(q) + \hat{A}^\dagger(q'))$$
$$[\hat{A}(q), \hat{A}(q')] = [\hat{A}^\dagger(q), \hat{A}^\dagger(q')] = 0 \quad (14)$$

$\hat{K}$ reduces to

$$\hat{K} = -\frac{\hbar^2\alpha^2}{8m}[\hat{A}^2(q) + \hat{A}^{\dagger 2}(q) - 2q\hat{I} + \hat{A}(q) + \hat{A}^\dagger(q) - 2\hat{A}^\dagger(q)\hat{A}(q)] \quad (15)$$

Likewise, powers of $e^{-\alpha(\hat{x}-x_0)}$ appearing in the potential energy operator are obtained starting from eq 11. For example

$$\begin{aligned} e^{-2\alpha(\hat{x}-x_0)} &= \frac{1}{(2s+1)^2}\{4q^2\hat{I} - 4q[\hat{A}^\dagger(q) + \hat{A}(q)] + \\ &\quad \hat{A}^2(q) + \hat{A}^{\dagger 2}(q) + \hat{A}(q)\hat{A}^\dagger(q) + \hat{A}^\dagger(q)\hat{A}(q)\} \\ &= \frac{1}{(2s+1)^2}\{2(2q^2 + q)\hat{I} - (4q+1)[\hat{A}^\dagger(q) + \\ &\quad \hat{A}(q)] + 2\hat{A}^\dagger(q)\hat{A}(q) + \hat{A}^2(q) + \hat{A}^{\dagger 2}(q)\} \end{aligned} \quad (16)$$

Thus, the Morse potential term reads

$$\begin{aligned} (\upsilon(\hat{x}))^2 &= \frac{1}{(2s+1)^2}\{2(2q^2 + q)\hat{I} - (4q+1)[\hat{A}^\dagger(q) + \\ &\quad \hat{A}(q)] + 2\hat{A}^\dagger(q)\hat{A}(q) + \hat{A}^2(q) + \hat{A}^{\dagger 2}(q)\} - \\ &\quad \frac{2}{(2s+1)}\{2q\hat{I} - [\hat{A}^\dagger(q) + \hat{A}(q)]\} \\ &= \frac{1}{(2s+1)^2}\{(4q^2 - 2q - 8sq)\hat{I} + (4s - 4q + 1) \times \\ &\quad [\hat{A}^\dagger(q) + \hat{A}(q)] + 2\hat{A}^\dagger(q)\hat{A}(q) + \hat{A}^2(q) + \hat{A}^{\dagger 2}(q)\} \end{aligned} \quad (17)$$

Accordingly, the Morse Hamiltonian $\hat{H}_M = \hat{K} + a_2(\upsilon(\hat{x}))^2$ is expressed in algebraic form as

$$\begin{aligned} \hat{H}_M &= \left[\frac{2a_2}{(2s+1)^2} + \frac{\hbar^2\alpha^2}{4m}\right]\hat{A}^\dagger(q)\hat{A}(q) + \\ &\quad q\left[\frac{2a_2}{(2s+1)^2}(2q - 1 - 4s) + \frac{\hbar^2\alpha^2}{4m}\right]\hat{I} + \\ &\quad \left[\frac{a_2}{(2s+1)^2}(4s - 4q + 1) - \frac{\hbar^2\alpha^2}{8m}\right][\hat{A}^\dagger(q) + \hat{A}(q)] + \\ &\quad \left[\frac{a_2}{(2s+1)^2} - \frac{\hbar^2\alpha^2}{8m}\right][\hat{A}^2(q) + \hat{A}^{\dagger 2}(q)] \end{aligned} \quad (18)$$

The representation of eq 18 shows that the Morse Hamiltonian is generally 5-band diagonal on a GQNSB of the form in eq 3. We stress that the expression (eq 18) holds for any choice of parameters s and q, regardless of them being connected to any specific physical constraint.

If the condition

$$\frac{a_2}{(2s+1)^2} = \frac{\hbar^2\alpha^2}{8m} \quad (19)$$

(equivalent to eq 6) is satisfied, then the last term, proportional to $[\hat{A}^2(q) + \hat{A}^{\dagger 2}(q)]$ drops from $\hat{H}_M$. In other words, the choice of the parameter s of eq 6 makes the Morse Hamiltonian tridiagonal on the corresponding GQNSB basis, irrespective of q. Under this special condition (eq 18), the Morse Hamiltonian simplifies to

$$\hat{H}_M = \frac{4a_2}{(2s+1)^2}\{[\hat{A}^\dagger(q) + \hat{A}(q)](s - q) + \hat{A}^\dagger(q)\hat{A}(q) + (q^2 - 2qs)\hat{I}\} \quad (20)$$

The form of eq 20 indicates that by further setting

$$q = s \tag{21}$$

the operator form of the Hamiltonian simplifies even more, and the Morse Hamiltonian factorizes as

$$\hat{H}_{\mathrm{M}} = 4\frac{a_2}{(2s+1)^2}[\hat{A}^{\dagger}(s)\hat{A}(s) - s^2\hat{I}] \tag{22}$$

which recovers the algebraic form of the Morse Hamiltonian of previous works.[1,2]

The use of different values of q and s produces a GQNSB, where the algebraic computation of the matrix elements of the Hamiltonian (eq 2) is not significantly more intricate; in particular, on a GQNSB, the Morse Hamiltonian is 5-band diagonal, rather than tridiagonal,[9] and higher powers of $(v(x))^k$ in eq 1 generate $(2k + 1)$ band diagonal matrices (like in the QNSB).

For practical potentials, usually substantially distorted from the pure-Morse $(v(x))^2$ term, the actual eigenfunctions can be represented poorly by the $[s] + 1$ Morse bound states or, equivalently, by their QNSB counterparts; to achieve a good convergency of all eigenfunctions, the QNSB often needs to be complemented by a large number of states, far beyond $[s] + 1$. A suitably chosen GQNSB can thus prove significantly more efficient, especially in a multioscillator polyatomic context.

4. GQNSB Parametric Dependency

The shape of the wave functions (eq 3) depends on the four parameters x_0, α, s, and σ; different shapes imply different convergence properties when employed to build the matrix representation of the Hamiltonian. A brief analysis of the dependency of the shape of the GQNSB states on the various parameters can be useful to gain some insight into their role.[10] Figure 1 shows the profile of three states of the form in eq 3, under the conditions of eqs 5 and 6. Note that the $n = 0$ state is located substantially at the right of the Morse equilibrium position x_0 and that further states move in toward x_0 for increasing n. This contrasts with the behavior of a basis of energy eigenstates of a well centered in x_0. Figure 2 illustrates the behavior of a GQNSB wave function, eq 3, after variation of the parameters s and σ involved relative to the QNSB values, eqs 5 and 6. The dependence on the s parameter (Figure 2a) is weak; by increasing s, the eigenfunction shifts almost rigidly toward the outer region. The σ dependence (Figure 2b) is less trivial; for larger σ, the wave function deforms and shrinks, concentrating toward the region of the minimum and decaying more rapidly at large x. The role of the σ parameter is particularly important; as the nth GQNSB wave function (eq 3) has the general form

$$\phi_n(y) \propto \mathrm{e}^{-y/2}y^{\sigma}\mathrm{Pol}[y, n] \tag{23}$$

(Pol[y,n] stands for a polynomial of degree n in the variable y), σ controls the decay rate of the wave functions for $y \to 0$, that is, at the dissociation region. In particular, by choosing a small σ, the basis wave functions spread away from the well region, thus improving the convergency of high-energy states, possibly at the expense of quality of the low-energy states in the well. Equation 23 and Figure 2 show that the general shape and, in particular, the amount of localization of the GQNSB wave functions can be tuned freely by choosing suitable s and σ parameters; this allows improvement of the variational efficiency of a truncated GQNSB for a specific quantum mechanical problem.

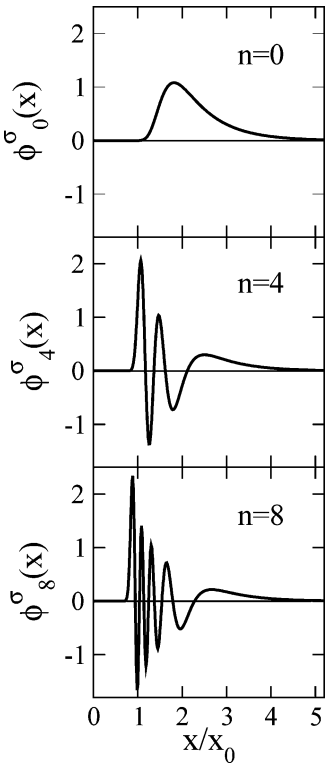

Figure 1. QNSB wave functions, for $n = 0$, 4, and 8, compatible with a Morse problem characterized by $x_0 = 1$, $\alpha = 4/x_0$, and $a_2 = 625$, in units where $\mu = 1$ and $\hbar = 1$ so that $s = 8.34$ and $\sigma = 0.34$.

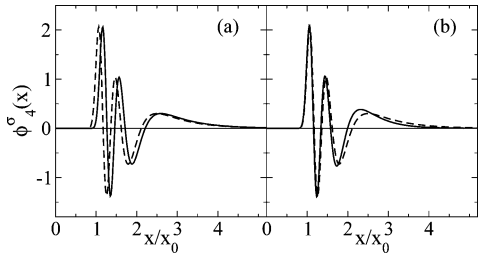

Figure 2. Variation of the $n = 4$ GQNSB wave function for a 50% increase in the parameters s (a) or σ (b), solid line, with respect to the QNSB starting wave function (dashed line), corresponding to $s = 8.34$, $\sigma = 0.34$, $x_0 = 1$, and $\alpha = 4/x_0$, like that in Figure 1.

5. Optimization of the Basis Parameters

Assume that the exact N_{b} bound-state eigenvalues E_i^{ex} of the Hamiltonian are known; we can measure the rms discrepancy of the discrete spectrum due to basis incompleteness by

$$\tilde{\Delta}^2 = \frac{1}{N_{\mathrm{b}}}\sum_{n=0}^{N_{\mathrm{b}}-1}(E_n - E_n^{\mathrm{ex}})^2 \tag{24}$$

in terms of the numerical eigenvalues E_i, obtained by diagonalizing the matrix of $\hat{H}$, eq 2, on a finite GQNSB composed of the first N_{s} ($> N_{\mathrm{b}}$) states and parametrized by s and σ. For fixed N_{s}, we can search for the optimal $s_{\min}$ and $\sigma_{\min}$ that make $\tilde{\Delta}$ minimum.

In fact, the a priori knowledge of the exact eigenvalues E_i^{ex} is not necessary; due to the variational nature of basis truncation, a "better" basis makes all eigenvalues E_i lower. Accordingly, the optimal $s_{\min}$ and $\sigma_{\min}$ parameters can be defined as those

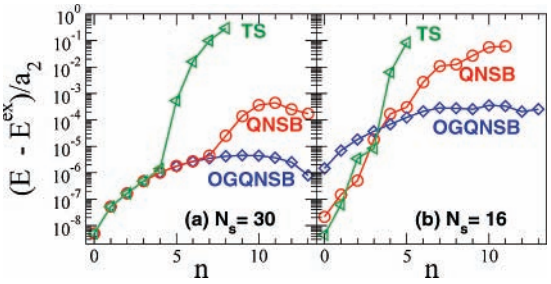

Figure 3. Discrepancies $(E_n - E_n^{ex})/a_2$ of the individual eigenvalues n for the potential $V(x) = a_2[(v(x))^2 + (v(x))^4]$. (a) $N_s = 30$ (OGQNSB with $s_{min} = 20.01$, $\sigma_{min} = 0.435$); and (b) $N_s = 16$ (OGQNSB with $s = 14.47$, $\sigma = 0.314$), for all bound states. The OGQNSB (diamonds) discrepancies are compared to those based on the QNSB (circles) and to the GQNSB based on the choice of (s,σ) made by Tennyson and Sutcliffe[4,5] (triangles).

producing the lowest eigenvalue spectrum for the assigned basis size N_s, that is, those minimizing

$$\Delta = \frac{1}{N_b}\sum_{n=0}^{N_b-1} E_n \qquad (25)$$

This approach only requires that the number N_b of bound eigenstates is known. Of course, the number N_b of bound states can be determined once and for all, for example, by means of a calculation on a very extended QNSB. The minimization of $\tilde{\Delta}$ and of Δ leads generally to slightly different results, but the following qualitative discussion applies equally well to both schemes. Unless specified, for the determination of s_{min} and σ_{min}, we minimize Δ as defined in eq 25 and compare Δ to its fully converged value Δ_0 computed on a largely complete basis.

In a typical application of the GQNSB, one starts from a molecular potential energy expressed in terms of an expansion of the form of eq 1. Before considering realistic dimers (H_2 and Ar_2), we illustrate the properties of the optimized GQNSB for a simple model potential defined by

$$N_{max} = 4 \quad a_2 = a_4 = 625 \quad a_3 = 0 \quad \alpha = 4 \quad x_0 = 1 \qquad (26)$$

which we solve combined with a kinetic term specified by $\hbar = 1$ and $\mu = 1$. We minimize Δ with respect to s and σ for two fixed numbers of basis states $N_s = 30$ and 16. Figure 3a shows the values of the individual eigenvalue discrepancy $(E_n - E_n^{ex})/a_2$ for the potential in eq 26, for the QNSB, for an optimized GQNSB (OGQNSB), and for a GQNSB with s and σ chosen according to the prescription of TS.[4,5] That prescription represents the basis used as the starting point of the optimization process employed by TS;[4,5] in those works, the optimization was performed over parameters equivalent to x_0 and α. We are not interested here in comparing the accuracy of different optimized basis but rather to study the convergency properties of a GQNSB with given s and σ and with the same x_0 and α values.[10] The optimized parameters of the $N_s = 30$ OGQNSB are $s_{min} = 20.01$ and $\sigma_{min} = 0.435$, to be compared with the QNSB ones, $s = 8.338$ and $\sigma = 0.338$, and those chosen according to the prescription of TS,[4,5] $s = 8.338$ and $\sigma = 9$. For this potential, $\Delta_0 = -444.90$, and the corresponding $\Delta - \Delta_0$ values are 3×10^{-6} for the OGQNSB (Δ equaling Δ_0 to five decimal digits), 0.061 for the QNSB, and 457 for the TS choice. Both QNSB and the OGQNSB retrieve all of the bound states, but the OGQNSB produces much better converged eigenenergies, especially near dissociation. The TS basis instead yields only 9 of the 14 bound states, only a few of which are converged within $10^{-2}a_2$, which explains the large discrepancy of $\Delta - \Delta_0$.

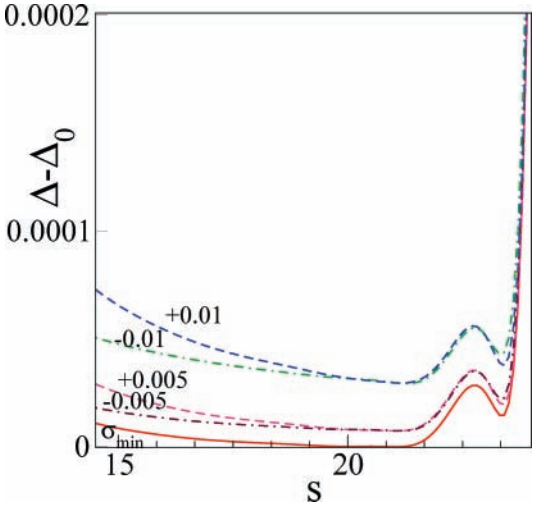

Figure 4. The s dependence of Δ, eq 25, for $V(x)$ defined in eq 26, computed with the GQNSB of $N_s = 30$ elements as a function of s, and for σ fixed to σ_{min}, to $\sigma_{min} \pm 0.005$, and to $\sigma_{min} \pm 0.01$.

Figure 3b shows the same individual discrepancies obtained with a basis of $N_s = 16$ states instead of 30. The s and σ values of the QNSB and the TS basis are, of course, unchanged, while for the OGQNSB, they change to $s_{min} = 14.47$ and $\sigma_{min} = 0.314$. The discrepancies $\Delta - \Delta_0$ deteriorate to 0.106, 87.35, and 4045.9 for OGQNSB, QNSB, and TS, respectively. Clearly, the OGQNSB maintains a fair accuracy throughout the spectrum by allowing for slightly less accurate lowest bound states, at the benefit of those near dissociation. In contrast, the $N_s = 16$ QNSB fails in obtaining the two bound states closest to dissociation, and the TS basis only produces six bound states. Thus, basis parameter optimization allows a substantial improvement of the accuracy of the results, with the same computational cost. In other words, the convergence speed of the computation can be improved drastically by means of a suitable choice of s and σ; for example, Figure 3 demonstrates an equal accuracy of the OGQNSB of 16 states and the QNSB of 30 states.

Figure 4 illustrates a typical s dependence of the total discrepancy $\Delta - \Delta_0$; for σ equal to its optimal value σ_{min} (solid curve), as s approaches the optimal s_{min} value from below, Δ decreases relatively slowly, while for s increasing beyond s_{min}, Δ grows very steeply. The σ dependence of Δ has a sharp and roughly symmetrical deep minimum around σ_{min}.

The reason for the observed s and σ dependencies of Δ is related to the GQNSB wave function profiles of Figures 1 and 2 and eq 23. When s increases, the GQNSB wave functions shift almost rigidly toward the dissociation region of the potential. As the GQNSB wave functions decay much more rapidly for small x than for large x, approaching s_{min} from below the accuracy of the representation of the bound states localized in the well region improves slowly, but soon after the optimal s is found, all wave functions move their localization region to the right of the equilibrium position and cease to account well for the eigenstates behavior at the left of x_0. On the other hand, σ affects mainly the vanishing rate for large x, which affects the bound-state representation quite severely, but in a rather symmetric way. Convergency can be quite substantially improved by tuning the wave function localization, and this can be achieved by choosing the most appropriate s and σ, thus precisely the OGQNSB.

TABLE 1: Fit Quality and Parameters for a Model Potential (eq 1), $N_{max} = 8$, to the Ar_2 Potential

δ_{RMS}	0.26 E_h
δ_{RMS} well	0.48 cm^{-1}
α	$0.516787 a_0^{-1}$
a_2	1359.70868 μE_h
a_3	1136.96625 μE_h
a_4	181.96578 μE_h
a_5	−43.51541 μE_h
a_6	3.77230 μE_h
a_7	−0.13914 μE_h
a_8	0.00202 μE_h
x_0	$7.116 a_0$

TABLE 2: Energy Differences (in cm^{-1}) between Consecutive $J = 0$ Vibrational Levels of Ar_2

$i - i'$	numerical[a]	OGQNSB $N_s = 100$	experiment[b]
1 − 0	25.76	25.64	25.69
2 − 1	20.49	20.43	20.58
3 − 2	15.44	15.46	15.58
4 − 3	10.79	10.90	10.91
5 − 4	6.75	6.92	6.84
6 − 5	3.56	3.71	
7 − 6	1.36	1.31	

[a] Numerical diagonalization of the Patkowski et al. potential.[11] [b] Ultraviolet laser spectroscopy data by Herman et al.[13]

6. Examples of Applications

The simple model potential of section 5 allowed us to investigate the main properties of the optimized basis and the role of parameters s and σ. After that quite artificial model, we apply the present basis optimization method to two real dimers, Ar_2 and H_2. These two very different 1D problems are good testing grounds for evaluating the basis performance. We do not aim at especially accurate spectroscopic results, which we obtain nonetheless, despite the simplicity of our treatment.

6.1. Ar_2. We compare the OGQNSB and the QNSB for the calculation of the vibrational spectrum of the Argon dimer, for which a reliable ab initio molecular potential is provided[11] in terms of a set of 47 points in the range of $x = 0.25-20$ Å. Patkowski et al.[11] propose an analytic expression fitting the ab initio points rather accurately. We fit the ab initio data instead to the expansion of eq 1, up to degree $N_{max} = 8$. The resulting best-fit coefficients are reported in Table 1. Since the repulsive small-x region does not affect the bound states significantly anyway, we focus on the convergence inside of the binding well region, with a weighted fit.[12] Despite its simplicity, generality, and the relatively small number of parameters involved ($N_{max} + 1 = 9$), the resulting expansion is quite accurate throughout the whole energy range covered by the 47 ab initio points. In particular, in the well region, the agreement is quite good, with a rms discrepancy δ_{RMS} of less than 0.5 wavenumbers; see Table 1. Moreover, the resulting model potential does not suffer from the unphysical small-x divergence to $-\infty$ of the fitted function[11] and rather tracks the repulsive region within a few electronvolts. The well depth (classical dissociation energy) is

$$D_e = \sum_{i=2}^{N_{max}} (-)^i a_i = 99.23 \text{ cm}^{-1}$$

We apply the algebraic method and solve the resulting quantum mechanical problem (eq 2) for the bound-state eigenvalues, using QNSB and GQNSB of different size N_s. Table 2 compares the results obtained by the finite-differences solution of the Schrödinger equation for the analytic potential by Patkowski et al.[11] and by numerical diagonalization of the algebraic Hamiltonian (eq 2) with the parameters from Table 1 on a large $N_s = 100$ OGQNSB ($s = 80.18$, $\sigma = 0.213$). This large OGQNSB was chosen to ensure that the results were fully converged and is taken as reference. The excitation energies obtained using our expansion compare favorably to those obtained by using the analytical expression by Patkowski et al.[11] and to the experimental $J = 0$ data,[13] demonstrating equally good or better agreement.

TABLE 3: Bound-State Eigenvalues of the Ar_2 Dimer, Computed with Different Methods, All Based on the Ab Initio Values[11] [in cm^{-1}]

state	OGQNSB $N_s = 100$	QNSB $N_s = 100$	QNSB $N_s = 20$	QNSB $N_s = 15$
0	−84.41	−84.41 (−)	−84.41 (−)	−84.40 (0.005)
1	−58.77	−58.77 (−)	−58.77 (−)	−58.75 (0.01)
2	−38.34	−38.34 (−)	−38.34 (−)	−38.31 (0.02)
3	−22.88	−22.88 (−)	−22.88 (−)	−22.84 (0.04)
4	−11.98	−11.98 (−)	−11.98 (−)	−11.93 (0.05)
5	−5.06	−5.06 (−)	−5.06 (−)	−5.02 (0.04)
6	−1.35	−1.35 (−)	−1.35 (−)	−1.32 (0.02)
7	−0.036	−0.015 (0.02)	*0.022 (0.06)*	*0.051 (0.09)*

Table 3 illustrates the convergency properties of the unoptimized QNSB by reporting the eigenvalues obtained by diagonalizing the expanded Hamiltonian (eq 2) on $N_s = 100$, 20, and 15 states. The energy differences with respect to the $N_s = 100$ OGQNSB reference are shown, in parentheses, when exceeding 10^{-3} cm^{-1}. Fairly well converged results are obtained even for the small $N_s = 15$ QNSB. Notice however that the bound state closest to dissociation is unbound for $N_s = 15$ and 20 since it is so extended that a rather large QNSB ($N_s \geq 42$) is needed to obtain it at negative energy. Even the very large $N_s = 100$ QNSB does not provide a well-converged result for that specific level.

By diagonalizing the expanded Hamiltonian (eq 2) on $N_s = 20$ and 15 OGQNSB, we obtain the complete spectrum, and with an accuracy $\Delta - \Delta_0$ of 6×10^{-5} and 0.013 cm^{-1}, respectively. The accuracy of all bound levels but the last one is basically the same as that for the corresponding QNSB, but the complete discrete spectrum is obtained, including the highest level. The accuracy of the $N_s = 15$ OGQNSB is therefore better than that of $N_s = 100$ QNSB for Ar_2. Reducing the basis size below $N_s = 15$, the highest state is missing, but the GQNSB can still be tuned to obtain a fair accuracy of all other states ($\Delta - \Delta_0 < 0.5 cm^{-1}$ for $N_s \geq 11$).

6.2. H_2. In a previous work,[1] we applied the QNSB formalism to the ab initio adiabatic potential[14,15] for the H_2 molecule. We found that an expansion (eq 1) up to $N_{max} = 12$ fits all 169 available ab initio points with a deviation $\delta_{RMS} = 5.5$ cm^{-1}. This expansion, whose parameters are reported in Table 4 of ref 1, produces all of the 15 vibrational bound states of this molecule. The QNSB parameters for this potential are $s = 25.56$ and $\sigma = 0.564$. The QNSB produces a wavenumber-converged spectrum using $N_s \geq 28$ basis states.[16]

By minimizing $\tilde{\Delta}$, eq 24, we generate an OGQNSB of smaller N_s. For the calculation of $\tilde{\Delta}$, we use the fully converged $N_s = 200$ QNSB results as reference, reported in the second column of Table 4. An $N_s = 25$ OGQNSB with $s = 26.36$ and $\sigma = 2.115$ ($\tilde{\Delta} = 0.173$ cm^{-1}) produces eigenvalues with the same wavenumber figures, that is, the same accuracy of the $N_s = 28$ QNSB; since they are identical to the second column of Table 4, they are not shown. For less strict accuracy requirements, one could reduce the basis size; the last two columns of Table 4 compare the eigenvalues obtained with $N_s = 21$ QNSB and

TABLE 4: H_2 Bound-State Energies in Reduced-Size Algebraic Bases; in Parentheses are the Differences with Respect to the Reference [in cm^{-1}]

state	QNSB[a] $N_s = 200$	QNSB[b] $N_s = 21$	OGQNSB[c] $N_s = 21$
0	−36113	−36113 (−)	−36113 (−)
1	−31948	−31948 (−)	−31948 (−)
2	−28020	−28019 (1)	−28020 (−)
3	−24324	−24322 (2)	−24324 (−)
4	−20856	−20845 (11)	−20856 (−)
5	−17614	−17573 (41)	−17614 (−)
6	−14599	−14486 (113)	−14598 (1)
7	−11815	−11588 (227)	−11814 (2)
8	−9271	−8907 (365)	−9269 (3)
9	−6979	−6486 (493)	−6975 (4)
10	−4955	−4376 (579)	−4951 (4)
11	−3222	−2626 (596)	−3218 (4)
12	−1810	−1281 (530)	−1806 (5)
13	−761	−389 (372)	−757 (4)
14	−135	−9 (126)	−125 (10)

[a] Reference fully converged calculation. [b] Eigenvalues obtained with an $N_s = 21$ QNSB. The maximum difference of 596 cm^{-1} corresponds to 1.6% of the well depth. [c] Eigenvalues obtained with an $N_s = 21$ OGQNSB ($s = 23.52$ and $\sigma = 3.194$). The maximum difference of 10 cm^{-1} corresponds to 0.03% of the well depth.

OGQNSB. The H_2 potential expansion illustrates the robustness of the GQNSB in state-poor situations; here, for the $N_s = 21$ QNSB eigenvalues, the differences with respect to the fully converged values reach hundreds of wavenumbers, with a rms discrepancy of $\tilde{\Delta} = 323$ cm^{-1}, while the discrepancy of the eigenvalues obtained by diagonalizing on the $N_s = 21$ OGQNSB amounts to $\tilde{\Delta} = 3.7$ cm^{-1} only.

7. Conclusions

The substantial improvement of the variational accuracy of the bound-state spectra computed on a OGQNSB with respect to the unoptimized QNSB permits, in practice, calculations of a given accuracy on a significantly smaller basis size to be made. While this improvement is practically irrelevant to the solution of the one-dimensional vibrational problem of diatomics, it is of great importance for the application of this method to the calculation of the spectra based on the ab initio multidimensional potential surfaces of polyatomic molecules, as is currently pursued in quantum chemical research.[17−22] In particular, the OGQNSB approach can be incorporated easily into most present-day Morse-coordinate-based codes for computing vibrational spectra of polyatomic molecules.[4,5,23−25] We are also currently developing a custom implementation of a generalization of the expansion in eq 1 to the polyatomic case,[26] to be solved in a multidimensional OGQNSB.

Acknowledgment. We thank Konrad Patkowski for kindly providing us with the complete ab initio Ar_2 PES data, including those not available in his paper.[11]

References and Notes

(1) Bordoni, A.; Manini, N. *Int. J. Quantum Chem.* **2007**, *107*, 782.

(2) Molnár, B.; Földi, P.; Benedict, M. G.; Bartha, F. *Europhys. Lett.* **2003**, *61*, 445.

(3) Lemus, R.; Arias, J. M.; Gómez-Camacho, J. *J. Phys. A: Math. Gen.* **2004**, *37*, 1805.

(4) Tennyson, J.; Sutcliffe, B. T. *J. Chem. Phys.* **1982**, *77*, 4061.

(5) Tennyson, J.; Kostin, M. A.; Barletta, P.; Harris, G. J.; Polyansky, O. L.; Ramanlal, J.; Zobov, N. F. *Comput. Phys. Commun.* **2004**, *163*, 85.

(6) Cooper, F.; Khare, A.; Sukhatme, U. P. *Phys. Rep.* **1995**, *251*, 268.

(7) One could even consider different q for the A and $A^\dagger$ operators, but such a more general choice does not seem particularly interesting for molecular applications; we take a single q.

(8) The use of an α basis parameter different from the potential one affects the matrix elements substantially. This is seen through the recursive relations for the matrix elements,[2] specialized to the present case (subscript B and P stand for basis and potential respectively), $\langle\phi_m|e^{-(\alpha_P/\alpha_B)\alpha_B(\hat{x}-x_0)}|\phi_{n+1}\rangle = [C_m\langle\phi_{m-1}|e^{-(\alpha_P/\alpha_B)\alpha_B(\hat{x}-x_0)}|\phi_n\rangle + (n - m - (\alpha_P/\alpha_B))\langle\phi_m|e^{-(\alpha_P/\alpha_B)\alpha_B(\hat{x}-x_0)}|\phi_n\rangle]/C_{n+1}$ and $\langle\phi_0|e^{-(\alpha_P/\alpha_B)\alpha_B(\hat{x}-x_0)}|\phi_0\rangle = [\Gamma(2\sigma + (\alpha_P/\alpha_B))]/[(2s + 1)^{(\alpha_P/\alpha_B)}\Gamma(2\sigma)]$, where the C_n are the coefficients of eq 10. This recursion implies that if $\alpha_P \neq k\alpha_B$ for integer k, all matrix elements of integer powers of $e^{-\alpha_P(\hat{x}-x_0)}$ are nonvanishing. Moreover, these recursive relations are more intricate than the algebraic rules holding when α_P/α_B is an integer.

(9) In addition, eqs 5 and 6 grant an isomorphism of the Morse problem bound-state subspace with the subspace generated by the first $[s] + 1$ states of the QNSB;[2] this isomorphism does not hold for the general s and σ.

(10) The shape and convergency properties of the basis are affected also by x_0 and α; for example, TS[4,5] varied both parameters for their basis optimization. In contrast, here we keep α fixed to the value derived from the potential expansion to preserve the matrix sparseness and fix x_0 to the equilibrium position of the potential; we show that allowing s and σ to vary provides a sufficient basis flexibility to improve the convergency substantially.

(11) Patkowski, K.; Murdachaew, G.; Fou, C.-M.; Szalewicz, K. *Mol. Phys.* **2005**, *103*, 2031.

(12) We weight all data points below dissociation proportionally to $1/(100cm^{-1})^2 (\simeq 1/(D_e)^2)$ and those above dissociation proportionally to $1/(100V_j^2)$, where V_j is the ab initio adiabatic energy of the jth data point.

(13) Herman, P. R.; LaRoque, P. E.; Stoicheff, B. P. *J. Chem. Phys.* **1988**, *89*, 4535.

(14) Schwartz, C.; Le Roy, R. J. *J. Mol. Spectrosc.* **1987**, *121*, 420.

(15) Kolos, W.; Wolniewicz, L. *J. Chem. Phys.* **1968**, *49*, 404.

(16) A wavenumber accuracy seems to be a low resolution compared to current spectroscopic standards, but (i) it is sufficient to show the difference in performance of different bases; (ii) the interpolating potential suffers from a larger RMS deviation; and (iii) nonadiabatic and relativistic corrections, neglected in the present model, affect the vibrational levels in the 10 cm^{-1} range.[14,15]

(17) Wyatt, R. *J. Chem. Phys.* **1998**, *109*, 10732.

(18) Pochert, J.; Quack, M.; Stohner, J.; Willeke, M. *J. Chem. Phys.* **2000**, *113*, 2719.

(19) Callegari, A.; Pearman, R.; Choi, S.; Engels, P.; Srivastava, H.; Gruebele, M.; Lehmann, K. K.; Scoles, G. *Mol. Phys.* **2003**, *101*, 551.

(20) Handy, N. C.; Carter, S. *Mol. Phys.* **2004**, *102*, 2201.

(21) Zobov, N. F.; Ovsyannikov, R. I.; Shirin, S. V.; Polyansky, O. L. *Opt. Spectrosc.* **2007**, *102*, 348.

(22) Makarewicz, J.; Skalozub, A. *J. Phys. Chem. A* **2007**, *111*, 7860.

(23) Spirko, V.; Jensen, P.; Bunker, P. R.;Cejchan, A. *J. Mol. Spectrosc.* **1985**, *112*, 183.

(24) Jensen, P. *J. Mol. Spectrosc.* **1988**, *128*, 478.

(25) Jensen, P. *Mol. Phys.* **2000**, *98*, 1253.

(26) Bordoni, A. Calculation of Molecular Vibrational Spectra through a Complete Morse Expansion. Ph.D. Thesis, University of Milan, 2006, http://www.mi.infm.it/manini/theses/BordoniPhD. pdf, Chapter 6.